Chapter 11

Complex-Valued Generalized Hebbian Algorithm and Its Applications to Sensor Array Signal Processing

Yanwu Zhang

Principal component extraction is an efficient statistical tool that is applied to feature extraction, data compression, and signal processing. The Generalized Hebbian Algorithm (GHA) (Sanger 1992) can be used to iteratively extract principal eigenvectors in the real domain. In some scenarios such as sensor array signal processing, we encounter complex data. The Complex-valued Generalized Hebbian Algorithm (CGHA) (Zhang *et al.* 1997) is presented in this chapter. Convergence of CGHA is proved. Like GHA, CGHA can be implemented by a single-layer linear neural network. An application of CGHA to sensor array signal processing is demonstrated through Direction of Arrival (DOA) estimation.

1 Review of Principal Component Extraction and the Generalized Hebbian Algorithm (GHA)

Consider the autocorrelation matrix of an N-dimensional random column vector X: $R_{XX} = E[XX^H]$ where H stands for conjugate transpose. R_{XX} can be expressed as (Strang 1993):

$$R_{XX} = \sum_{i=1}^{N} \lambda_i U_i U_i^H \tag{1}$$

where U_i is the ith eigenvector (column vector) and λ_i is the corresponding eigenvalue. Here the eigenvectors are normalized and orthogonalized. In the real domain, conjugate transpose H reduces to transpose T.

If we sort the eigenvectors by their associated eigenvalues in descending order, the leading eigenvectors are called the principal eigenvectors because they span the major portion of R_{XX}.

Due to their statistical significance, principal eigenvectors find applications in various realms. Their usefulness to sensor array signal processing will be demonstrated in Section 3.

Data compression also relies on principal eigenvectors. The technique of principal component extraction (also called principal component analysis) (Sanger 1992), (Oja 1992), (Haykin 1994) linearly reduces the dimensionality of input data while retaining major statistical information (Bannour *et al.* 1995), (Plumbley 1995), shown as follows.

Consider an N-dimensional zero-mean random vector

$$X = [x_1 \quad x_2 \quad \cdots \quad x_N]^T \tag{2}$$

We desire to reduce its dimension from N to M ($M < N$). First, we find the M principal eigenvectors of the input's autocorrelation matrix R_{XX}, denoted as $U_1, U_2, \cdots, U_M$ (orthonormalized and arranged in descending order of their associated eigenvalues). These column vectors constitute an $N \times M$ mapping matrix

$$Q = [U_1 \ \vdots \ U_2 \ \vdots \ \cdots \ \vdots \ U_M] \tag{3}$$

Then we map the N-dimensional input vector X to an M-dimensional output vector Y through Q:

$$Y = Q^H X \tag{4}$$

Elements of vector Y are called principal components.

Since $M < N$, dimensionality of the input vector space is reduced. Data are thus compressed. Compression generally induces information loss, but it can be proven (Hornik *et al.* 1992) that the linear transform in Equation (4) is optimal in the sense that it minimizes the mean squared error when reconstructing X:

$$\hat{X} = QY \tag{5}$$

Sanger presented the Generalized Hebbian Algorithm (GHA) (Sanger 1992) to iteratively derive principal eigenvectors using a single-layer linear neural network. The algorithm can be summarized as follows.

The $N \times 1$ input vector X is expressed in Equation (2). The eigenvectors of R_{XX} are denoted as $U_1, U_2, \cdots, U_N$ (arranged in descending eigenvalue order). We randomly initialize $N \times 1$ vectors $V_1, V_2, \cdots, V_N$. GHA then updates V_j iteratively. The updating rule for V_j at iteration step n is given by Equation (6) and Equation (7):

$$V_j(n+1) = V_j(n) + \mu(n) y_j(n) [X(n) - y_j(n) V_j(n) - \sum_{i<j} y_i(n) V_i(n)] \tag{6}$$

$$y_j(n) = V_j^T(n)X(n) \tag{7}$$

where $\mu(n)$ is a learning rate factor. Sanger proved that V_j converges to U_j (Sanger 1992).

GHA possesses the following features: snapshot-based processing instead of eigendecomposition, parallel processing, and good expandability. Hence this algorithm facilitates fast and distributed processing. It has been applied to image coding and texture segmentation (Sanger 1992).

2 Complex-Valued Generalized Hebbian Algorithm (CGHA)

GHA is applicable only in the real domain. In some scenarios, we encounter complex data. For example, in sensor array signal processing, typically the received real signal at each sensor is quadrature demodulated to a complex signal (Van Trees 2002). We are interested in the principal eigenvectors of the array's autocorrelation matrix because they contain key information about the signals' incoming directions. Therefore, an extension of GHA to the complex domain is needed.

2.1 Formulation of CGHA

Now we present the Complex-valued Generalized Hebbian Algorithm (CGHA) (Zhang *et al.* 1997). Randomly initialize $N \times 1$ vectors $V_1, V_2, \cdots, V_N$. CGHA then updates V_j iteratively. The updating rule for V_j at iteration step n is given by Equation (8) and Equation (9):

$$V_j(n+1) = V_j(n) + \mu(n) y_j^*(n)[X(n) - y_j(n)V_j(n) - \sum_{i<j} y_i(n)V_i(n)] \tag{8}$$

$$y_j(n) = V_j^H(n)X(n) \tag{9}$$

where $y_j^*(n)$ denotes the complex conjugate of $y_j(n)$, and $\mu(n)$ is a learning rate factor. $V_j(n)$ will converge to the jth normalized eigenvector of R_{XX}. Proof is given in the next subsection.

As shown in Figure 1, each block represents an N-dimensional weight vector V_j $(j = 1, 2, \cdots, N)$. The output of the jth block is $y_j = V_j^H X$. As the input vector X flows through each block, $y_j V_j$ is subtracted from X to form the updating vector that is contained in the bracket in Equation (8).

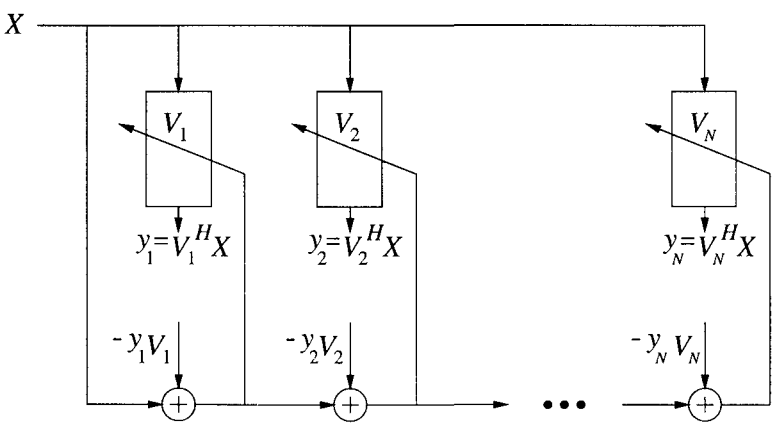

Figure 1. Implementation of CGHA.

2.2 Convergence of CGHA

Convergence analysis of CGHA extends that of GHA (Sanger 1992) to the complex domain. Let us rewrite Equation (8) in matrix form to include all eigenvectors:

$$W(n+1) = W(n) + \mu(n)\Big\{X(n)X^H(n)W(n) - W(n)\{UT[Y(n)Y^H(n)]\}\Big\} \quad (10)$$

where $W(n)$ is an $N \times N$ matrix:
$W(n) = [V_1(n) \ \vdots \ V_2(n) \ \vdots \ \cdots \ \vdots \ V_N(n)]$, and

$$Y(n) = W^H(n)X(n) \quad (11)$$

Operator $UT[\cdot]$ (standing for upper triangle) sets all elements below the diagonal of the square matrix to zero, thereby producing an upper triangular matrix.

Assume temporal stationarity. Then $R_{XX} = E[X(n)X^H(n)]$ does not vary with n. Taking expectation on both sides of Equation (10) and incorporating Equation (11), we have

$$W(n+1) = W(n) + \mu(n)\Big\{R_{XX}W(n) - W(n)\{UT[W^H(n)R_{XX}W(n)]\}\Big\} \quad (12)$$

The convergence property of the above discrete-time difference equation is the same as that of the following continuous-time differential equation:

$$\frac{d}{dt}W(t) = R_{XX}W(t) - W(t)\{UT[W^H(t)R_{XX}W(t)]\} \quad (13)$$

We prove the convergence in two steps:

§1 Prove that $V_1(t)$ converges to the eigenvector associated with the largest eigenvalue.

V_1 is the first column of matrix W. According to Equation (13), variation of $V_1(t)$ is governed by

$$\frac{d}{dt}V_1(t) = R_{XX}V_1(t) - V_1(t)[V_1^H(t)R_{XX}V_1(t)] \tag{14}$$

Assume R_{XX} is positive definite with N distinct eigenvalues $\lambda_1 > \lambda_2 > \cdots > \lambda_N$ which correspond to orthonormalized eigenvectors $E_1, E_2, \cdots, E_N$. Note that since R_{XX} is Hermitian, all of its eigenvalues are real.

Expand $V_1(t)$ as

$$V_1(t) = \sum_{k=1}^{N} c_k(t)E_k \tag{15}$$

E_k $(k = 1, 2, \cdots, N)$ is an orthonormal base. Premultiply E_k^H to both sides of Equation (15) and we have

$$c_k(t) = E_k^H V_1(t) \tag{16}$$

Plugging Equation (16) together with $R_{XX}E_k = \lambda_k E_k$ into Equation (14) gives

$$\sum_{k=1}^{N} \frac{dc_k(t)}{dt}E_k = \sum_{k=1}^{N} c_k(t)\lambda_k E_k - [\sum_{l=1}^{N} |c_l(t)|^2\lambda_l] \sum_{k=1}^{N} c_k(t)E_k \tag{17}$$

where $|\cdot|$ denotes norm of a complex variable.

Premultiply E_k^H to both sides of Equation (17). The orthonormality of base E_k leads to

$$\frac{dc_k(t)}{dt} = c_k(t)[\lambda_k - \sum_{l=1}^{N} |c_l(t)|^2\lambda_l] \tag{18}$$

We now study the convergence of $c_k(t)$ in two cases: when $k > 1$ and when $k = 1$.

(a) When $k > 1$.

Define $r_k(t) = \frac{c_k(t)}{c_1(t)}$, assuming $c_1(t) \neq 0$. Take differentiation of $r_k(t)$ with respect to t:

$$\frac{dr_k(t)}{dt} = \frac{1}{c_1(t)}[\frac{dc_k(t)}{dt} - r_k(t)\frac{dc_1(t)}{dt}] \tag{19}$$

Plugging Equation (18) into Equation (19), we have

$$\begin{aligned}\frac{dr_k(t)}{dt} &= \frac{1}{c_1(t)}\Big\{c_k(t)[\lambda_k - \sum_{l=1}^{N}|c_l(t)|^2\lambda_l] \\ &\quad -r_k(t)c_1(t)[\lambda_1 - \sum_{l=1}^{N}|c_l(t)|^2\lambda_l]\Big\}\end{aligned} \tag{20}$$

which can be simplified to

$$\frac{dr_k(t)}{dt} = r_k(t)(\lambda_k - \lambda_1) \tag{21}$$

The solution to the above differential equation is

$$r_k(t) = r_k(0)\, e^{(\lambda_k - \lambda_1)t} \tag{22}$$

We know that $\lambda_k < \lambda_1$ for $k > 1$. Therefore, with any initial value, $r_k(t)$ exponentially decays to 0 when $k > 1$.

(b) When $k = 1$.

According to Equation (18) and definition $r_k(t) = \frac{c_k(t)}{c_1(t)}$, we have

$$\frac{dc_1(t)}{dt} = c_1(t)[\lambda_1 - |c_1(t)|^2\lambda_1 - |c_1(t)|^2\sum_{l=2}^{N}|r_l(t)|^2\lambda_l] \tag{23}$$

We have shown that $r_k(t)$ exponentially decays to 0 when $k > 1$. So at a large t, $|c_1(t)|^2\lambda_1$ dominates over $|c_1(t)|^2 \sum_{l=2}^{N} |r_l(t)|^2\lambda_l$. For convergence analysis, we can thus drop the last term. Then Equation (23) reduces to

$$\frac{dc_1(t)}{dt} = c_1(t)[\lambda_1 - |c_1(t)|^2\lambda_1] \tag{24}$$

Let us define another function

$$F(t) = [|c_1(t)|^2 - 1]^2 \tag{25}$$

Utilizing Equation (24), we have

$$\frac{dF(t)}{dt} = -4\lambda_1|c_1(t)|^2[|c_1(t)|^2 - 1]^2 \tag{26}$$

Equation (25) gives that $F(t) \geq 0$, and Equation (26) shows that $\frac{dF(t)}{dt} \leq 0$. Therefore $F(t)$ must converge to 0. Equivalently, $|c_1(t)|$ converges to 1, according to Equation (25).

By Equation (15) and definition $r_k(t) = \frac{c_k(t)}{c_1(t)}$, we have $V_1(t) = c_1(t)E_1 + c_1(t)\sum_{k=2}^{N} r_k(t)E_k$. In 1a, it is shown that $r_k(t)$ converges to 0 when $k > 1$. In 1b it is shown that $|c_1(t)|$ converges to 1. Hence $V_1(t)$ converges to E_1 with a complex factor of norm one.

§2 Prove that for $j > 1$, $V_j(t)$ converges to the eigenvector associated with the jth largest eigenvalue.

We resort to the method of induction. Given that $V_1(t) \to E_1$, we only need to show that if $V_k(t)$ converges to E_k for $k = 1, 2, \cdots, j-1$, $V_j(t)$ converges to E_j.

According to Equation (13), variation of $V_j(t)$ is governed by

$$\frac{d}{dt}V_j(t) = R_{XX}V_j(t) - \sum_{k\leq j} V_k(t)[V_k^H(t)R_{XX}V_j(t)] \tag{27}$$

$V_k(t)$ can be expressed as

$$V_k(t) = E_k + \epsilon_k(t)G_k(t) \tag{28}$$

where $G_k(t)$ is a unit-length vector and $\epsilon_k(t)$ is a scalar.

The premise of the induction is that $V_k(t)$ converges to E_k for $k < j$, so $\epsilon_k(t)$ converges to 0 for $k < j$. Combining Equation (28) and Equation (27), we have

$$\begin{aligned} \frac{d}{dt}V_j(t) &= R_{XX}V_j(t) - V_j(t)[V_j^H(t)R_{XX}V_j(t)] \\ &\quad - \sum_{k<j} E_k[E_k^H(t)R_{XX}V_j(t)] \\ &\quad + O(\epsilon) + O(|\epsilon|^2) \end{aligned} \tag{29}$$

where $O(\epsilon)$ represents a term converging to 0 at least as fast as the slowest vanishing $\epsilon_k(t)$ for $k < j$. $O(|\epsilon|^2)$ has a similar meaning. At a large t, we neglect terms $O(\epsilon)$ and $O(|\epsilon|^2)$.

Expand $V_j(t)$ as

$$V_j(t) = \sum_{k=1}^{N} b_k(t)E_k \tag{30}$$

where $b_k(t) = E_k^H V_j(t)$

Plugging Equation (30) together with $R_{XX}E_k = \lambda_k E_k$ into Equation (29) (neglecting vanishing terms), we have

$$\begin{aligned} \sum_{k=1}^{N} \frac{db_k(t)}{dt}E_k &= -\sum_{k<j}[\sum_{l=1}^{N} |b_l(t)|^2\lambda_l]b_k(t)E_k \\ &\quad + \sum_{k=j}^{N}[\lambda_k - \sum_{l=1}^{N} |b_l(t)|^2\lambda_l]b_k(t)E_k \end{aligned} \tag{31}$$

Premultiplying E_k^H to both sides of Equation (31), and utilizing the orthonormality of E_k, we have

$$\frac{db_k(t)}{dt} = -b_k(t)\sum_{l=1}^{N}|b_l(t)|^2\lambda_l \qquad \text{for } k < j \tag{32}$$

$$\frac{db_k(t)}{dt} = b_k(t)[\lambda_k - \sum_{l=1}^{N}|b_l(t)|^2\lambda_l] \qquad \text{for } k \geq j \tag{33}$$

(a) For $k < j$, the solution to differential equation (32) is

$$b_k(t) = b_k(0)e^{-[\sum_{l=1}^{N}|b_l(t)|^2\lambda_l]t} \tag{34}$$

R_{XX} is positive definite, so $\lambda_l > 0$. Hence $-[\sum_{l=1}^{N}|b_l(t)|^2\lambda_l] < 0$. Consequently, $b_k(t)$ exponentially decays to 0 for $k < j$.

(b) For $k > j$, define $s_k(t) = \frac{b_k(t)}{b_j(t)}$, assuming $b_j(t) \neq 0$. Then Equation (33) leads to

$$\begin{aligned}\frac{ds_k(t)}{dt} &= \frac{1}{b_j(t)}\{b_k(t)[\lambda_k - \sum_{l=1}^{N}|b_l(t)|^2\lambda_l] \\ &\quad -s_k(t)b_j(t)[\lambda_j - \sum_{l=1}^{N}|b_l(t)|^2\lambda_l]\}\end{aligned} \tag{35}$$

which can be simplified to

$$\frac{ds_k(t)}{dt} = s_k(t)(\lambda_k - \lambda_j) \tag{36}$$

The solution to the above differential equation is

$$s_k(t) = s_k(0)e^{(\lambda_k - \lambda_j)t} \tag{37}$$

Since $\lambda_k < \lambda_j$ for any $k > j$, $s_k(t)$ exponentially decays to 0 for $k > j$.

(c) For $k = j$, Equation (33) becomes

$$\frac{db_j(t)}{dt} = b_j(t)[\lambda_j - |b_j(t)|^2\lambda_j - |b_j(t)|^2 \sum_{l>j} |s_l(t)|^2\lambda_l - \sum_{l<j} |b_l(t)|^2\lambda_l] \quad (38)$$

It has been shown in 2a that $b_l(t) \to 0$ for $l < j$, and in 2b that $s_l(t) \to 0$ for $l > j$. We thus drop the last two terms in Equation (38) for a large t, and the equation reduces to

$$\frac{db_j(t)}{dt} = b_j(t)[\lambda_j - |b_j(t)|^2\lambda_j] \quad (39)$$

To show that $b_j(t)$ converges, we define another function

$$H(t) = [|b_j(t)|^2 - 1]^2 \quad (40)$$

Using Equation (39), we have

$$\frac{dH(t)}{dt} = -4\lambda_j|b_j(t)|^2[|b_j(t)|^2 - 1]^2 \quad (41)$$

Equation (40) gives that $H(t) \geq 0$, and Equation (41) shows that $\frac{dH(t)}{dt} \leq 0$. Therefore $H(t)$ must converge to 0. Equivalently, $|b_j(t)|$ converges to 1, according to Equation (40).

We know the expansion $V_j(t) = b_j(t)E_j + \sum_{k<j} b_k(t)E_k + \sum_{k>j} b_k(t)E_k$. It has been shown that $b_k(t) \to 0$ for $k < j$, $b_k(t) \to 0$ for $k > j$ (because $s_k(t) \to 0$ for $k > j$), and $|b_j(t)| \to 1$. Therefore $V_j(t)$ converges to E_j with a complex factor of norm one.

Analyses in §1 and §2 establish convergence of CGHA: $V_j(n)$ converges to E_j for $j = 1, 2, \cdots, N$.

2.3 Implementation of CGHA

As illustrated in Figure 1, CGHA can be implemented by a single-layer linear neural network. The slanted arrows in the figure represent updating of V_j, $j = 1, 2, \cdots, N$.

Like GHA, CGHA possesses the following features:

§1 There is no need to estimate the autocorrelation matrix R_{XX}. Its eigenvectors are derived directly from the input vector. In sensor array signal processing, the input vector is just a snapshot of received signals at all sensors at one sampling instant.

§2 The implementation architecture has good expandability. Updating of V_j is affected by V_k of $k < j$, but not by V_k of $k > j$. If convergence has been reached for the first M eigenvectors, the additional learning of the $(M+1)$th eigenvector will leave intact the preceding M eigenvectors.

§3 The algorithm can be carried out by parallel processing. Equation (8) can be rewritten as

$$V_j(n+1) = V_j(n) + \mu(n) y_j^*(n)[X_j(n) - y_j(n)V_j(n)] \quad (42)$$

where

$$X_j(n) = X(n) - \sum_{i<j} y_i(n)V_i(n) \quad (43)$$

can be deemed the "net" input for updating V_j.

Equation (42) gives a uniform rule for updating V_j. Thus CGHA can be carried out by multiple processors in parallel.

3 Application of CGHA to Sensor Array Signal Processing

3.1 Transformation of Real Signal to Complex Signal by Quadrature Demodulation

Consider a linear array composed of N equally spaced sensors with identical directivity. Suppose D narrowband signals impinge on the array as plane waves from directions $\theta_1, \theta_2, \cdots, \theta_D$, as illustrated in Figure 2. Assume the received noise is spatially white with zero mean, and is uncorrelated with the signals.

Suppose the narrow-band signals have a carrier frequency f_0. At sensor No. N, the received narrow-band signal of incident angle θ_k can be expressed as

$$s_{kN}(t) = f_k(t)cos[2\pi f_0 t + \phi_k(t)] \tag{44}$$

where amplitude $f_k(t)$ and phase $\phi_k(t)$ have narrow bands that satisfy (Van Trees 2002)

$$B_{f_k}\ \Delta T_k \ll 1 \tag{45}$$

$$B_{\phi_k}\ \Delta T_k \ll 1 \tag{46}$$

where B_{f_k} and B_{ϕ_k} are the bandwidth of $f_k(t)$ and $\phi_k(t)$, respectively. ΔT_k is the plane wave's travel time from sensor No. 1 to No. N. Hence variations of $f_k(t)$ and $\phi_k(t)$ over ΔT_k can be deemed negligible.

Relative to the signal received by sensor No. N, the received signal at sensor No. m ($m = 1, 2, \cdots, N-1$) has a time delay:

$$s_{km}(t) = f_k(t - \tau_{km})\, cos[2\pi f_0(t - \tau_{km}) + \phi_k(t - \tau_{km})] \quad (47)$$

where

$$\tau_{km} = \frac{[(N - m)d]sin(\theta_k)}{c} \quad (48)$$

is the delay; d is the spacing between adjacent sensors, and c is the propagation speed of the plane waves.

Under the narrow-band conditions in Equation (45) and Equation (46), we have

$$f_k(t - \tau_{km}) \approx f_k(t) \quad (49)$$
$$\phi_k(t - \tau_{km}) \approx \phi_k(t) \quad (50)$$

Then Equation (47) is simplified to

$$s_{km}(t) = f_k(t)\, cos[2\pi f_0(t - \tau_{km}) + \phi_k(t)] \quad (51)$$

The received signal is carried at a center frequency f_0. To lower the sampling frequency and hence reduce the system's cost, the signal is typically quadrature demodulated (Van Trees 2002) prior to analog-to-digital conversion. Quadrature demodulation is illustrated in Figure 2. Two branches of the received signal are multiplied by $2cos(2\pi f_0 t)$ and $-2sin(2\pi f_0 t)$, respectively, and then low-passed to keep only the base-band components. The two branches then add up to a complex base-band signal. After quadrature demodulation, real signal $s_{km}(t)$ in Equation (51) is transformed to a complex signal

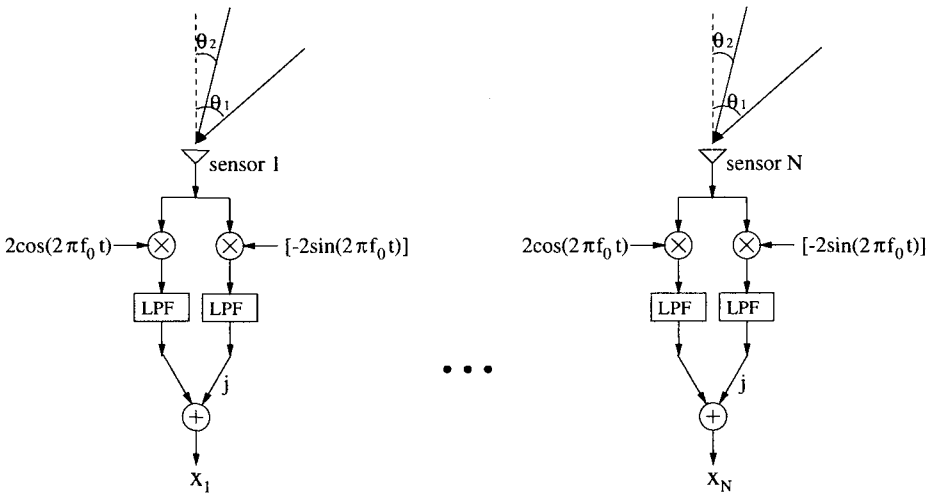

Figure 2. Quadrature demodulation of sensor array signals. At each sensor's output, the imaginary part (the right branch) is multiplied by j prior to summation.

$$\begin{aligned}\tilde{s}_{km}(t) &= f_k(t)\, cos[\phi_k(t) - 2\pi f_0 \tau_{km}] \\ &\quad + j\Big\{ f_k(t)\, sin[\phi_k(t) - 2\pi f_0 \tau_{km}] \Big\} \\ &= f_k(t)\, e^{j\phi_k(t)}\, e^{-j2\pi f_0 \tau_{km}} \end{aligned} \tag{52}$$

where the real part $f_k(t)cos[\phi_k(t) - 2\pi f_0 \tau_{km}]$ is called the in-phase component, and the imaginary part $f_k(t)sin[\phi_k(t) - 2\pi f_0 \tau_{km}]$ is called the quadrature component.

The original signal $s_{km}(t)$ can be restored from $\tilde{s}_{km}(t)$ by using both the in-phase and the quadrature components:

$$\begin{aligned} s_{km}(t) &= Re\{\tilde{s}_{km}(t)\, e^{j2\pi f_0 t}\} \\ &= Re\Big\{ [f_k(t)\, e^{j\phi_k(t)}\, e^{-j2\pi f_0 \tau_{km}}]\, e^{j2\pi f_0 t} \Big\} \end{aligned} \tag{53}$$

where $Re\{\cdot\}$ takes the real part of the argument.

Note that $s_{km}(t)$ cannot be restored by the in-phase component or the quadrature component alone. Hence we need to keep both components to preserve the information contained in $s_{km}(t)$. Complex signal $\tilde{s}_{km}(t)$ in Equation (52) is thus an equivalent representation of the original real signal $s_{km}(t)$.

3.2 Direction-Of-Arrival (DOA) Derived from Principal Eigenvectors of Array's Autocorrelation Matrix

Equation (52) gives the signals' phase-shift relationship between sensors. Now let us combine Equation (52) and Equation (48), and introduce notation

$$\gamma_k = \frac{f_0 d sin(\theta_k)}{c} \tag{54}$$

Then for the signal of incident angle θ_k, demodulated signals at all sensors can be expressed by an N-element column vector:

$$\begin{aligned} \tilde{S}_k(t) &= f_k(t)e^{j\phi_k(t)}[e^{-j2\pi f_0\tau_{k1}} \ \cdots \ e^{-j2\pi f_0\tau_{kN}}]^T \\ &= f_k(t)e^{j\phi_k(t)}[e^{-j2\pi(N-1)\gamma_k} \ \cdots \ e^{-j2\pi(N-N)\gamma_k}]^T \\ &= f_k(t)e^{j\phi_k(t)}e^{-j2\pi(N-1)\gamma_k}[1 \ \cdots \ e^{j2\pi(N-1)\gamma_k}]^T \\ &= \tilde{f}_k(t)Z_k \end{aligned} \tag{55}$$

where $\tilde{f}_k(t) = f_k(t)e^{j\phi_k(t)}e^{-j2\pi(N-1)\gamma_k}$

$$Z_k = \begin{bmatrix} 1 \\ e^{j2\pi\gamma_k} \\ \vdots \\ e^{j2\pi(N-1)\gamma_k} \end{bmatrix} \tag{56}$$

is the steering vector of the kth signal. It carries information of the signal's direction, yet is independent of t.

The sum of the D signals received by the array is

$$\begin{aligned} \tilde{S}(t) &= \sum_{k=1}^{D} \tilde{S}_k(t) \\ &= \sum_{k=1}^{D} \tilde{f}_k(t) Z_k \\ &= \left[Z_1 \vdots Z_2 \vdots \cdots \vdots Z_D \right] \begin{bmatrix} \tilde{f}_1(t) \\ \tilde{f}_2(t) \\ \vdots \\ \tilde{f}_D(t) \end{bmatrix} \end{aligned} \tag{57}$$

With addition of noise, the total output of the array is represented by an N-element column vector $X(t)$:

$$\begin{aligned} X(t) &= \tilde{S}(t) + \tilde{B}(t) \\ &= \left[Z_1 \vdots Z_2 \vdots \cdots \vdots Z_D \right] \begin{bmatrix} \tilde{f}_1(t) \\ \tilde{f}_2(t) \\ \vdots \\ \tilde{f}_D(t) \end{bmatrix} + \begin{bmatrix} \tilde{b}_1(t) \\ \tilde{b}_2(t) \\ \vdots \\ \tilde{b}_N(t) \end{bmatrix} \end{aligned} \tag{58}$$

where column vector $\tilde{B}(t) = [\tilde{b}_1(t)\ \tilde{b}_2(t)\ \cdots\ \tilde{b}_N(t)]^T$ denotes noise received by the N sensors. The noise is assumed to be spatially white with zero mean and variance σ^2, and uncorrelated with the signals.

The autocorrelation matrix of $X(t)$ is $R_{XX} = E[X(t)X^H(t)]$, an $N \times N$ matrix. Denote the eigenvectors as V_j, $j = 1, 2, \cdots, N$. Assuming the signals do not contain coherent pairs (Van Trees 2002), it can be shown (Schmidt 1986) that D eigenvectors have eigenvalues larger than σ^2. V_j $(j = 1, 2, \cdots, D)$ span the signal subspace (Van Trees 2002).

Signals' directions can be estimated from these principal eigenvectors (Tufts 1998). Utilizing properties of Vandermonde vectors (the steering vectors Z_k in Equation (56) are Vandermonde vectors), Reddi proposed a method (Reddi 1979) to estimate the signals' directions based on the signal-subspace eigenvectors.

It can be shown (Cadzow 1988) that the signal-subspace eigenvectors are linear combinations of Z_k, $k = 1, 2, \cdots, D$:

$$V_j = \sum_{k=1}^{D} \alpha_{jk} Z_k \qquad j = 1, 2, \cdots, D \text{ with } \lambda_j > \sigma^2 \tag{59}$$

where α_{jk} is a coefficient.

By Equation (54) and Equation (56), Z_k can be regarded as a sinusoid of spatial frequency $\gamma_k = \frac{f_0 d sin(\theta_k)}{c}$ and of length N. Then V_j $(j = 1, 2, \cdots, D)$ can be regarded as a one-dimensional sequence composed of multiple sinusoids.

Utilizing Equation (59), we look for signals' directions in three steps:

- Obtain the signal-subspace eigenvectors V_j $(j = 1, 2, \cdots, D)$ by CGHA.

- Find the frequency components γ_k $(k = 1, 2, \cdots, D)$ of V_j.
- Derive θ_k by relationship $\gamma_k = \frac{f_0 d sin(\theta_k)}{c}$ (Equation (54)).

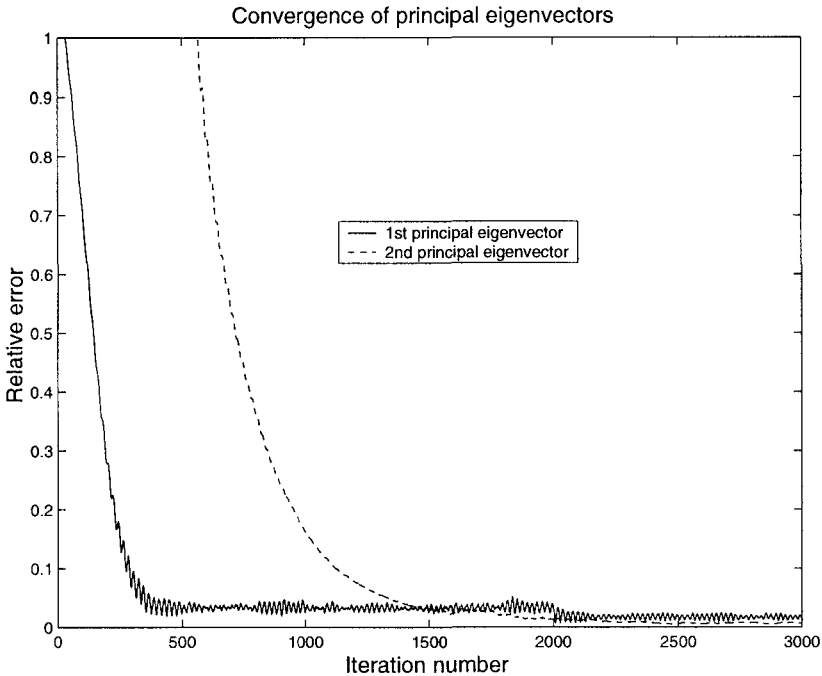

Figure 3. Learning curves of the first and the second principal eigenvectors.

Consider a 15-sensor uniform linear array. Two acoustic signals impinge on the array. The first signal is of normalized frequency $f_1 = 0.2$ (normalized by the sampling frequency) and incident angle $\theta_1 = 10°$. The second signal is of normalized frequency $f_2 = 0.15$ and incident angle $\theta_2 = 40°$. The sensor spacing is $d = \frac{1}{2}\lambda_1 = \frac{3}{8}\lambda_2$ where $\lambda_1 = \frac{c}{f_1}$ and $\lambda_2 = \frac{c}{f_2}$ are the wavelengths of the two signals, and c is the sound speed. Signal-to-Noise-Ratio (SNR) is 20 dB for

the first signal, and 14 dB for the second. Using demodulation frequency 0.2, the two signals are quadrature demodulated to $f_1' = 0$ and $f_2' = -0.05$, respectively.

Running CGHA, the simultaneous learning curves of the first and the second principal eigenvectors of R_{XX} are shown in Figure 3. The relative error of the kth principal eigenvector is defined as

$$\text{Relative error} = \frac{\| V_{k,precise} - V_{k,CGHA} \|}{\| V_{k,precise} \|} \tag{60}$$

where $V_{k,precise}$ is the precise eigenvector, and $V_{k,CGHA}$ is the eigenvector learned by CGHA. $\| \cdot \|$ denotes Euclidean norm. After 3000 iterations, the relative errors are 2% for the first principal eigenvector and 1% for the second. Using AutoRegressive (AR) modeling (Kay 1988) to analyze the principal eigenvectors obtained with CGHA, we get the spatial spectra of the first and the second principal eigenvectors, as shown in Figure 4.

With the first principal eigenvector, the two spectral peaks lie at spatial frequencies 0.087 and 0.240. By the spatial frequency definition in Equation (54), the peak frequencies correspond to direction estimates $\hat{\theta}_1 = 10.0°$ and $\hat{\theta}_2 = 39.8°$. With the second principal eigenvector, the two spectral peaks lie at spatial frequencies 0.085 and 0.241, corresponding to $\hat{\theta}_1 = 9.8°$ and $\hat{\theta}_2 = 40.0°$. These estimates are very close to the true values $\theta_1 = 10°$ and $\theta_2 = 40°$.

4 Conclusion

The Complex-valued Generalized Hebbian Algorithm (CGHA) is presented in this chapter. Its convergence is proved. The algorithm can be implemented by a single-layer linear neural network. An application of CGHA to sensor array signal processing is demonstrated. Converged principal eigenvectors provide good estimates of signals'

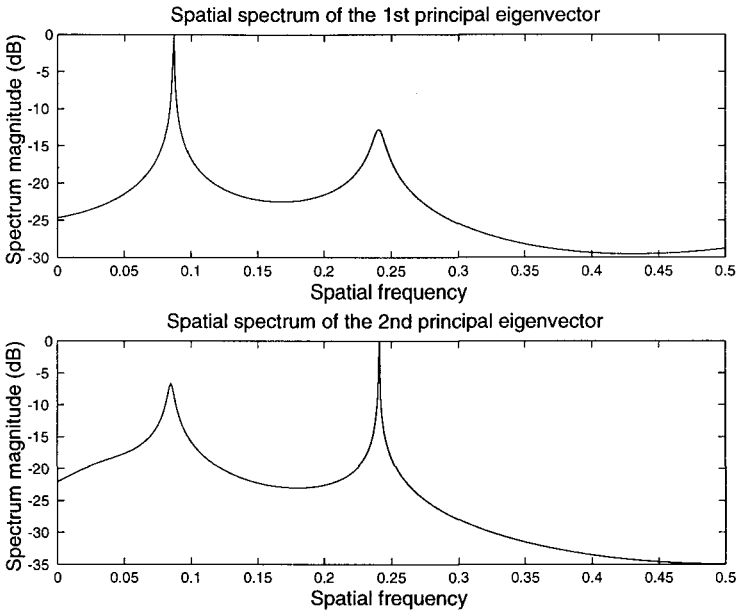

Figure 4. AR spectra of the first and the second eigenvectors.

directions.

Acknowledgment

CGHA was first presented in (Zhang *et al.* 1997). For developing Section 3 of this book chapter, the author thanks his MIT Ph.D. thesis advisor Prof. Arthur Baggeroer for the teaching in course "Sonar, Radar, and Seismic Signal Processing" for which the author was a teaching assistant. Sincere thanks go to Prof. Akira Hirose for offering the opportunity to incorporate the work into this book.

References

Bannour, S. and Azimi-sadjadi, M. (1995), "Principal Component Extraction Using Recursive Least Squares Learning," *IEEE Transactions on Neural Networks*, vol. 6, No. 2, pp. 457-469.

Cadzow, J. A. (1988), "A High Resolution Direction-of-Arrival Algorithm for Narrow-Band Coherent and Incoherent Sources," *IEEE Transactions on Acoustics, Speech, and Signal Processing*, vol. 36, No. 7, pp. 965-979.

Haykin, S. (1994), *Neural Networks: A Comprehensive Foundation*, Macmillan College Publishing Company, Inc., New York.

Hornik, K. and Kuan, C. (1992), "Convergence Analysis of Local Feature Extraction Algorithms," *Neural Networks*, vol. 5, No. 2. pp. 229-240.

Kay, S. M. (1988), *Modern Spectral Estimation: Theory and Application*, Prentice-Hall, Inc., Englewood Cliffs, NJ.

Oja, E. (1992), "Principal Components, Minor Components, and Linear Neural Networks," *Neural Networks*, vol. 5, No. 6, pp. 927-935.

Plumbley, M. (1995), "Lyapunov Functions for Convergence of Principal Component Algorithms," *Neural Networks*, vol. 8, No. 1, pp. 11-23.

Reddi, S. S. (1979), "Multiple Source Location - A Digital Approach," *IEEE Transactions on Aerospace and Electronic Systems*, , vol. AES-15, No. 1, pp. 95-105.

Sanger, T. D. (1992), "Optimal Unsupervised Learning in a Single-Layer Linear Feedforward Neural Network," *Neural Networks*, vol. 2, No. 6, pp. 459-473.

Schmidt, R. O. (1986), "Multiple Emitter Location and Signal Parameter Estimation," *IEEE Transactions on Antennas and Propagation*, vol. AP-34, No. 3, pp. 276-280.

Strang, G. (1993), *Introduction to Linear Algebra*, Wellesley-Cambridge Press, Wellesley, MA.

Tufts, D. W. (1998), "A Perspective on the History of Underwater Acoustic Signal Processing," *IEEE Signal Processing Magazine*, pp. 23-27, July.

Van Trees, H. L. (2002), *Optimum Array Processing*, John Wiley & Sons, Inc., New York.

Zhang, Y. and Ma, Y. (1997), "CGHA for Principal Component Extraction in the Complex Domain," *IEEE Transactions on Neural Networks*, vol. 8, No. 5, pp. 1031-1036.

Author's address

Yanwu Zhang: c/o Aware Inc., 40 Middlesex Turnpike, Bedford, MA 01730, U.S.A. Email: yanwu@alum.mit.edu